On the Most Adequate Round Notched Specimen for Hydrogen Embrittlement Testing

J. Toribio[1] and F. J. Ayaso[2]

[1] Department of Materials Engineering, University of Salamanca, Spain
[2] Department of Materials Science, University of La Coruña, Spain

ABSTRACT: *This paper studies a wide range of axisymmetric notched specimens in order to choose the most adequate geometry for measuring the hydrogen embrittlement susceptibility of metallic materials in the form of bar or wire, widely used in civil engineering. Since hydrogen transport by stress-assisted diffusion depends on both hydrogen concentration and hydrostatic stress distributions, the comparison between different geometries is performed on the basis of their distributions of hydrostatic stress calculated by an elastic-plastic finite element code and using the stress-strain law associated with a constitutive equation typical of a high-strength steel. The computations allow an analysis of the depth of the maximum hydrostatic stress point (place towards which hydrogen diffuses) and its evolution with time, these two being the key items for hydrogen transport by stress-assisted lattice diffusion. Finally, a discussion is presented about the advantages of notched geometries for hydrogen embrittlement testing and about the most adequate specimen considering its radial distribution of hydrostatic stress and its influence on hydrogen transport by diffusion. This will provide bases for further experimental analysis of the interactions between the stress-strain field in the material and hydrogen-assisted corrosion processes.*

INTRODUCTION

Many corrosion problems in a wide range of key industries are linked with environmentally assisted cracking (EAC) in its different forms. In fields of activities such as power, chemical and nuclear engineering hydrogen is frequently present as a consequence of electrochemical reactions or hydrogenous working agents. In this framework, the effect of hydrogen environments on fracture of metals has been well recognised as a significant source of risk of failure, and hydrogen diffusion has been proposed as the key transport mechanism controlling the phenomenon of hydrogen assisted cracking (HAC) or hydrogen embrittlement (HE).

Slow Strain Rate (SSR) testing is now a well recognised technique for measuring the susceptibility of metals to environmentally induced fracture, in spite of its inherent limitations regarding strain rate and potential

dependence. Development of this method has lead to the International Standard *ISO 7539-7* [1] which provides guidelines for this kind of EAC testing. A variety of specimens (initially plain, notched and pre-cracked) can be used (cf. [1]) but the advantages of notched samples in stress corrosion testing have been pointed out, and they are specially recommended for the analysis of hydrogen assisted fracture of metallic materials [2,3]. Thus the choice of the most adequate notched specimen is a problem of major technological concern for optimum HE testing in the industry.

PROBLEM STATEMENT

In HE processes, hydrogen transportation into prospective micro-damage sites in the fracture process zone comprises several sequential stages: environmental transport to metal, entry into it, and penetration through it. One of the main hydrogen transport mechanisms is lattice diffusion, as discussed elsewhere [4]. Diffusion equations based on both hydrogen concentration and hydrostatic stress distribution were proposed in the past [5,6]. They consist of the classical Fick´s equations modified with a term depending on the hydrostatic stress: hydrogen diffuses not only towards the points of minimum concentration, but also towards those places of maximum hydrostatic stress or, in other words, the sites of maximum hydrostatic strain, where there is more space to be filled by hydrogen. Thus the hydrogen flux density **J** depends on the gradients of concentration c and hydrostatic stress σ (σ = tr σ /3, where σ is the stress tensor):

$$\mathbf{J} = -D^* \, \mathbf{grad} \, c + Mc \, \mathbf{grad} \, \sigma \tag{1}$$

$$\partial c/\partial t = D^* \, \Delta c - M \, \mathbf{grad} \, c \cdot \mathbf{grad} \, \sigma - Mc \, \Delta \sigma \tag{2}$$

where t is the time, D* the hydrogen diffusion coefficient and M a second coefficient, a function of the first:

$$M = D^* V^* / RT \tag{3}$$

where V* is the molar partial volume of hydrogen, R the ideal gases constant and T the absolute temperature.

Thus the question of elucidating the most adequate notched geometries for HE testing is based on the analysis of hydrostatic stress distributions in the vicinity of the notch tip for each notched geometry, since the hydrostatic

stress gradient is relevant to determine the hydrogen diffusion flux according to equation (1). To this end, numerical computations by the finite element method in the elastic-plastic regime are performed on different notched geometries, as described in the next section of this paper.

NUMERICAL COMPUTATION

The numerical modelling, useful for the HE analysis, is based on real experimental results of fracture tests in air on axisymmetric notched specimens with very different notch geometries.

The stress-strain curves of the seven steels used in the computations appear in Figure 1.
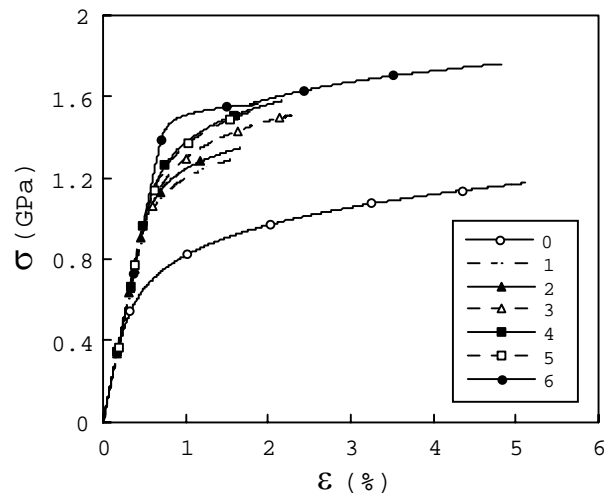

Figure 1: Stress-strain curves of the different steels.

Four notch geometries were used with each material. The dimensions of the specimens were the following:

- Geometry A : R/D = 0.03, C/D = 0.10
- Geometry B : R/D = 0.05, C/D = 0.30
- Geometry C : R/D = 0.40, C/D = 0.10
- Geometry D : R/D = 0.40, C/D = 0.30

where R is the notch radius, C the notch depth and D the external diameter of the specimen. These four notched geometries are depicted in Figure 2.
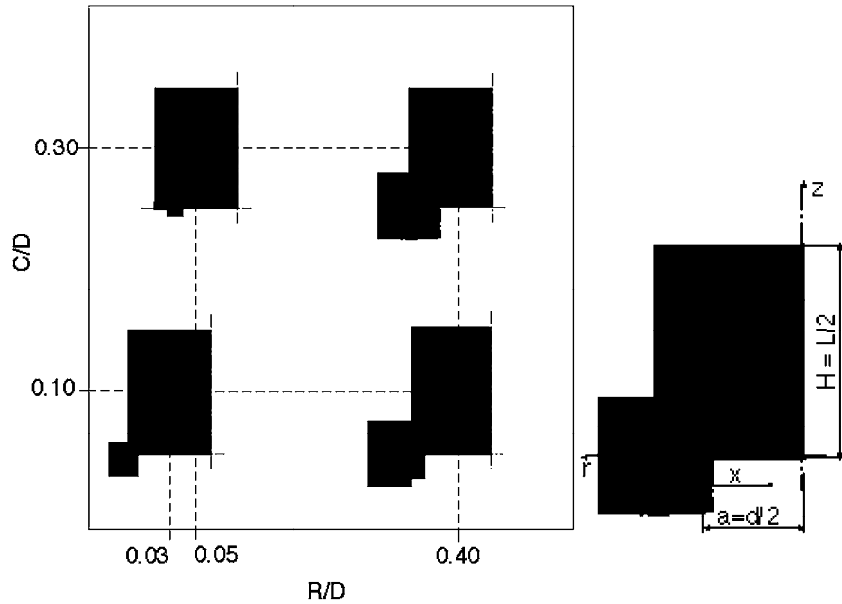
Figure 2: Notched geometries used in the experimental programme.

The finite element method (FEM) with an elastic-plastic code was applied, using a Von Mises yield surface. The external load was applied step by step, in the form of nodal displacements. An improved Newton-Raphson method was adopted, which modified the tangent stiffness matrix at each step. Large strains and large geometry changes were used in the computations by means of an updated lagrangian formulation, so as to predict the evolution of mechanical variables in the samples after the instant of maximum load (i.e, after the point of instability under load control), up to the instant of final failure by physical separation of the two fracture surfaces (i.e., up to the point of instability under displacement control).

The constitutive equation of the material —as a relationship between equivalent stress and strain— was introduced into the computer program from the real experimental results of the standard tension tests in the considered materials (see Figure 1). The curves were extended for large strains on the basis of the volume conservation in classical Plasticity and accounting for the strain hardening evolution to obtain steel 6 from the previous materials (steels 0 to 5).

The finite elements used in the computations were isoparametric with second-order interpolation (eight -node quadrilaterals and six-node triangles). The problem presents double symmetry, so as only a quarter of

the sample has to be analysed, and the displacements were fixed along the axes of symmetry (boundary conditions).

Figure 3 shows the four finite element meshes used in the computations associated with steel 0 and notched geometries A, B, C and D. The meshes used with steels 1 to 6 are similar to these, i.e., they have the same distribution of elements (the same topology as those used with steel 0) but their dimensions are proportional to the wire diameter in each particular case.
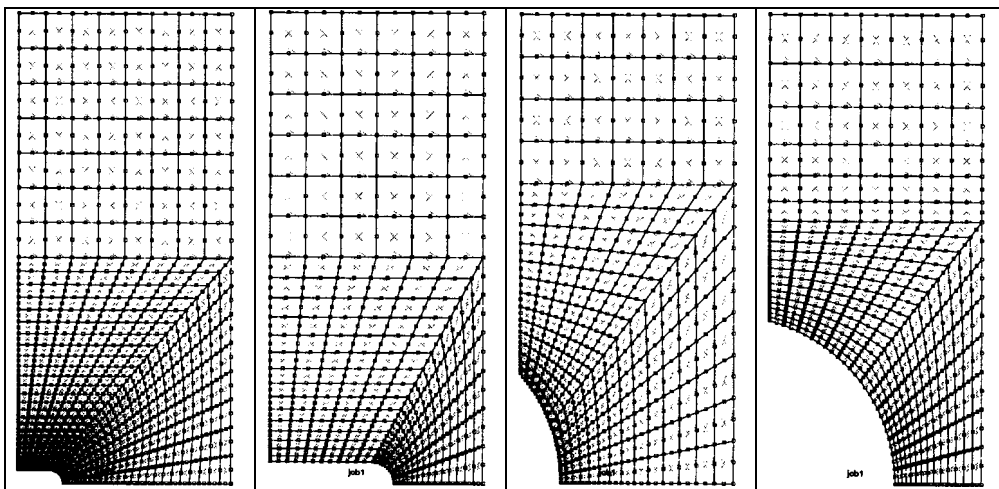

Figure 3: Finite element meshes used in the numerical computations. Those for steel 0 and geometries A, B, C and D are shown. Meshes for steels 1 to 6 are similar.

Figure 4 offers a comparison of the load-displacement curves really obtained in the fracture experiments and those numerically predicted by using the finite element method. Results for all geometries (A, B, C, D) and steel 0 are plotted. It is seen that the agreement can be considered as excellent in all cases, which indicates that the numerical modelling is accurate enough to predict the evolution of internal (continuum mechanics variables) in the specimens up to the final fracture moment of instability under displacement control, the numerical prediction of the load decrease part of the curve being also very good.
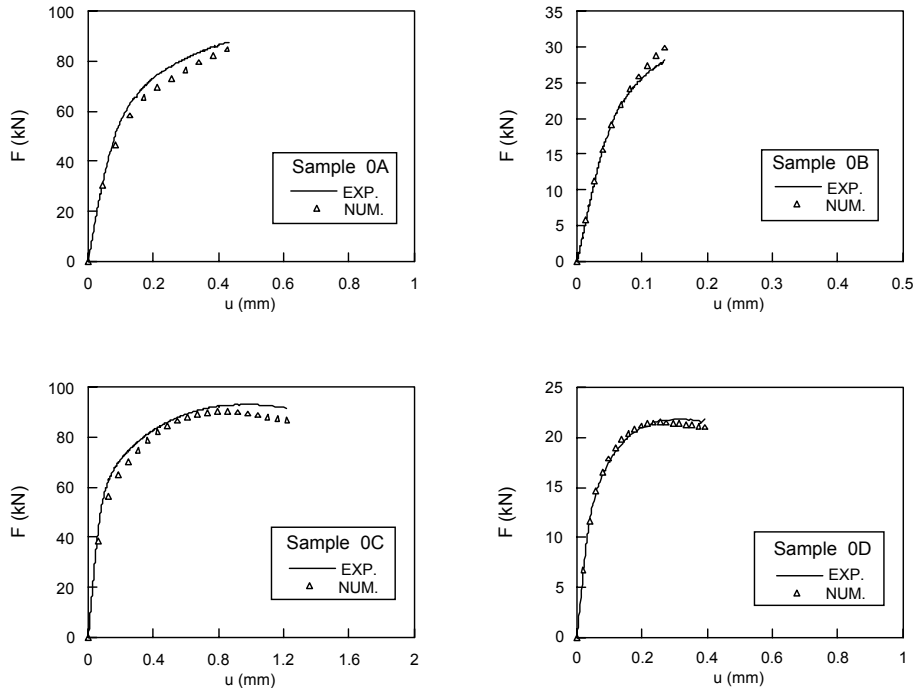
Figure 4: Experimental results (EXP) and numerical predictions (NUM) for steel 0.

RESULTS AND DISCUSSION

Figures 5 and 6 show the distributions of hydrostatic stress at instability point under load control (LC) and at the failure situation or instability point under displacement control (DC) for steels 0 and 6.

The hydrostatic stress reaches its maximum at certain distance from the notch tip in geometries A and B (those of minimum notch radius), and at the specimen axis in geometries C and D (those of maximum notch radius). In the latter case of notched specimens C and D there is a displacement of such a maximum hydrostatic stress point from the vicinity of the notch tip at the early steps of the loading process to the axis of the specimen at the latter steps of the loading process, including the load decrease part of the load-displacement curve after the instability point under load control (i.e., the point of maximum load).
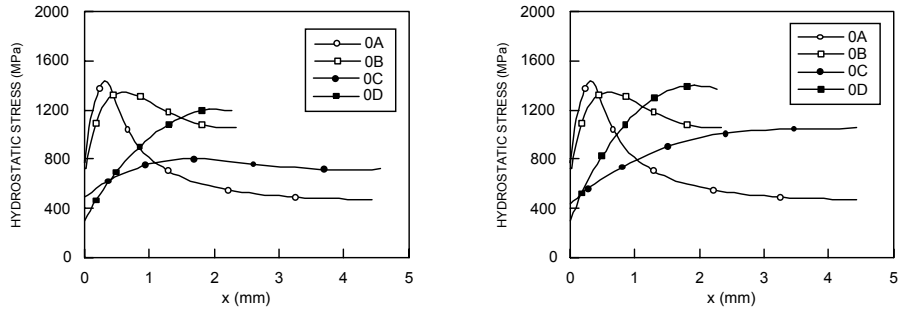
Figure 5: Hydrostatic stress distributions in notched samples A, B, C and D of steel 0, at the instants of LC instability (left) and DC instability (right).
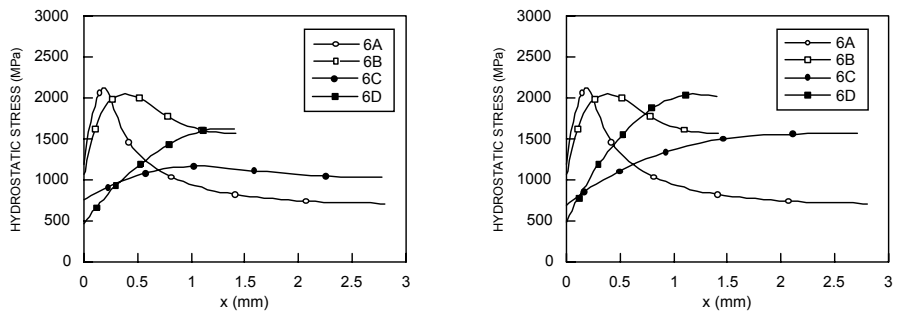

Figure 6: Hydrostatic stress distributions in notched samples A, B, C and D of steel 6, at the instants of LC instability (left) and DC instability (right).

The above results demonstrate, firstly, the advantages of notched specimens in HE testing, because the allow a "design" of certain *hydrostatic stress profile* governing the hydrogen entry and diffusion towards the prospective fracture places. The key items of such a profile are the hydrostatic stress at the notch tip σ_Γ (boundary condition for the hydrogen diffusion problem) and the hydrostatic stress gradient $(d\sigma/dx)$.

The hydrostatic stress profiles given in Figures 5 and 6 show no relevant shape differences between steels 0 and 6, i.e., the role of the constitutive equation of the material (given in the plots of Figure 1) is of minor importance regarding the gradient $d\sigma/dx$, although it is a key item in the matter of the magnitude of the hydrostatic stress levels, and particularly of the boundary value σ_Γ which is quite higher in the high strength steel 6 than

in the medium strength steel 0 and thus the former receives more hydrogen ingress than the latter.

The shape of the hydrostatic stress profile strongly depends on the notch geometry, this item being the key question of the present research. Sharp notch geometries A and B exhibit higher boundary values σ_Γ and higher gradients $d\sigma/dx$ than blunt notch specimens C and D, and therefore the former are more adequate for HE testing than the latter, since they allow a greater hydrogen entry and diffusion towards the critical areas and thus a better evaluation of HE susceptibility of materials. Considering the depth of the maximum hydrostatic stress point, geometry A (shallow notch) is the best to detect surface effects (maximum located near the notch tip), whereas geometry B (deep notch) is the best to analyse the hydrogen penetration towards the inner points.

With regard to the differences between LC and DC instability, they only appear in the case of geometries C and D whose load-displacement plots exhibit load decrease and thus an elevation of hydrostatic stress distributions takes place during the final part of the experiment. However, there is no significant alteration of the hydrostatic stress gradient ($d\sigma/dx$) and the same applies to the boundary value of the hydrostatic stress at the notch tip σ_Γ.

CONCLUSIONS

The performed numerical analysis of the hydrostatic stress distribution in notched geometries demonstrates that sharp notch specimens are the most adequate for hydrogen embrittlement testing, using either shallow notches to detect surface effects or deep notches to analyse hydrogen penetration.

REFERENCES

1. ISO 7539-7 (1989) Slow strain rate testing.
2. Thompson, A.W. (1985) *Materials Science and Technology* **1**, 711.
3. Toribio, J. and Elices, M. (1992) *Corrosion Science* **33**, 1387.
4. Toribio, J. (1997) *Materials Science and Engineering* **A219**, 180.
5. Van Leeuwen, H.P. (1974) *Engineering Fracture Mechanics* **6**, 141.
6. Astiz, M.A. (1987). In: *Computational Methods for Non Linear Problems*, Taylor, C., Owen, D.R.J. and Hinton, E. (Eds.). Pineridge Press, Swansea, pp. 271-299.